

Density functional theory study on the bridge structure in dimeric aluminum (III) water complexes

Qiang Miao, Qing Cao, and Shuping Bi^{a)}

State Key Laboratory of Coordination Chemistry, Department of Chemistry, Nanjing University, Nanjing 210093, People's Republic of China

(Received 4 March 2004; accepted 8 June 2004)

Density-functional theory methods were used to investigate the structure of dimeric aluminum (III) water complexes as a function of bridging group. The possibilities of oxygen, water, and hydroxyl bridge ligands and a variety of structural arrangements, such as *cis/trans*, with respect to the relative position of hydroxyl ligands, were considered. Within the limit of our computational level, we found that electrostatic repulsion between hydroxyls is important in deciding the polyaluminum structure. Although the structures of aluminum-hexaquo predominate, species with small number of charges or a large number of hydroxyl ligands have a tendency toward a five-coordinate trigonal bipyramidal configuration. Because water is electronically neutral, it cannot provide enough negative charges as a bridge ligand to stabilize two Al(III) molecules. The energy differences among many configurational isomers of hydroxyl Al are so small that they may coexist and convert into each other easily at room temperature. © 2004 American Institute of Physics.
[DOI: 10.1063/1.1778133]

I. INTRODUCTION

The aluminum(III)-water complex plays an important role in environmental chemistry.¹ It has many industrial applications that range from pharmaceutical design to the purification of water, and it can easily penetrate plants and cause Al(III) toxicity in both of them and in humans.^{2,3} However, the structure and configuration of polyaluminum has confused scholars for more than 100 years and has greatly hindered the progress of Al environmental chemistry and the industrial application of polyaluminum.¹ One of the intriguing problems about polyaluminum is the stability of candidate bridge ligands—including hydroxyl, oxygen, and water—and their configurationally isomerism. Although the results of previous experiments have indicated that the six-coordinate structure of hydroxyl aluminum should predominate,^{4,5} it is hard to demonstrate in the experimental setting whether the first hydration sphere should be octahedral, trigonal bipyramidal, or square pyramidal.⁶ However, the study of hydrated gas-phase metal ions can provide a link between the intrinsic chemistry of the isolated ion and its chemistry in solution by the aid of cluster calculations.^{7,8} Density functional theory calculation and *ab initio* molecular dynamics simulation have provided a theoretical perspective in understanding bridge structures in the Al(III)-water complex. So far, extensive theoretical studies have concentrated on the behavior of monomeric Al(III), especially the simplest species $\text{Al}(\text{H}_2\text{O})_6^{3+}$.⁹⁻¹⁴ They can provide important but limited information on bridge groups and the configuration of polynuclear Al. In this present paper, all possible configurations

of monomeric Al and bridge structures in dimeric Al-water complexes with different charges were considered. Within the limit of our computational level, we found that electrostatic repulsion between hydroxyls is important in the decision of polyaluminum structure. Although the structures of aluminum-hexaquo predominate, species with small number of charges or large number of hydroxyl ligands have a tendency toward a five-coordinate trigonal bipyramidal configuration. The electronically neutral water cannot provide enough negative charges as a bridge ligand to stabilize two Al(III). The energy differences among many configurational isomers of hydroxyl Al are so small that they may coexist and convert into each other easily at room temperature.

II. COMPUTATIONAL DETAILS

The model complexes that were used in the present study include $[\text{Al}(\text{H}_2\text{O})_6]^{3+}$, $[\text{Al}(\text{H}_2\text{O})_5\text{OH}]^{2+}$, $[\text{Al}(\text{H}_2\text{O})_4(\text{OH})_2]^+$, $[\text{Al}(\text{H}_2\text{O})_3(\text{OH})_3]^0$, $[\text{Al}(\text{OH})_4]^-$, $[\text{Al}_2(\text{OH})_2(\text{H}_2\text{O})_8]^{4+}$, $[\text{Al}_2(\text{OH})_3(\text{H}_2\text{O})_7]^{3+}$, $[\text{Al}_2(\text{OH})_4(\text{H}_2\text{O})_6]^{2+}$, $[\text{Al}_2(\text{OH})_5(\text{H}_2\text{O})_5]^+$, and $[\text{Al}_2(\text{OH})_6(\text{H}_2\text{O})_4]$. All possible configurations, with their corresponding hydroxyl, water, and oxygen bridge ligands, were calculated for comparison. Optimizations and frequency calculations were performed using the GAUSSIAN 98 program¹⁵ with density functional theory (DFT) at the B3LYP/6-31G+(*d,p*) level.^{16,17} Where possible, single point calculations using second-order Møller-Plesset (MP2) perturbation theory at the MP2/6-31G+(*d,p*) basis set were calculated for the purpose of comparison.¹⁸ A Berny algorithm using redundant internal coordinates was used in the geometry optimization.¹⁹ Atomic charges were calculated from natural population analyses (NPA), and wave functions

^{a)}Author to whom correspondence should be addressed. Permanent address: State Key Laboratory of Coordination Chemistry, Institute of Coordination Chemistry, Nanjing University, Nanjing 210093, People's Republic of China. Fax: 86-25-83317761. Electronic mail: bisp@nju.edu.cn

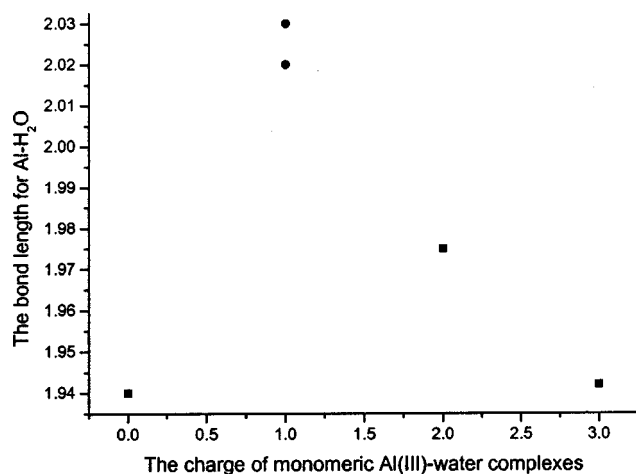
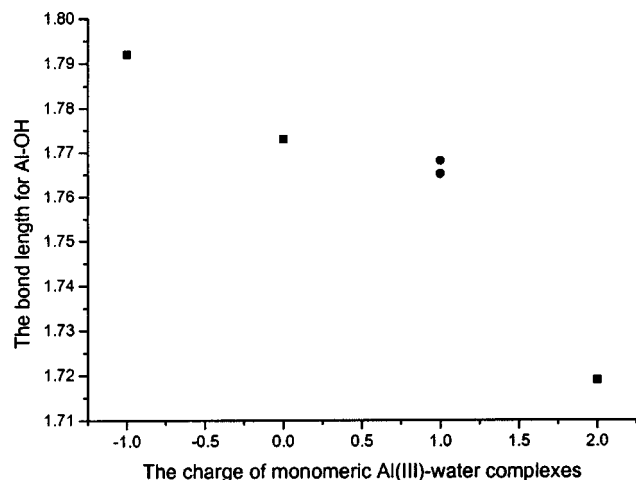


FIG. 1. The comparison of bond lengths and atomic charges between isomers and different species.

were analyzed using natural bond orbitals.^{20,21} The stability of all optimized species are confirmed by positive eigenvalues yielded in frequency calculations.

III. RESULTS AND DISCUSSION

A. Monomeric Al: The basic unit of polyaluminum

Monomeric hydroxyl Al(III) water complexes have configurational isomers because of the different relative posi-

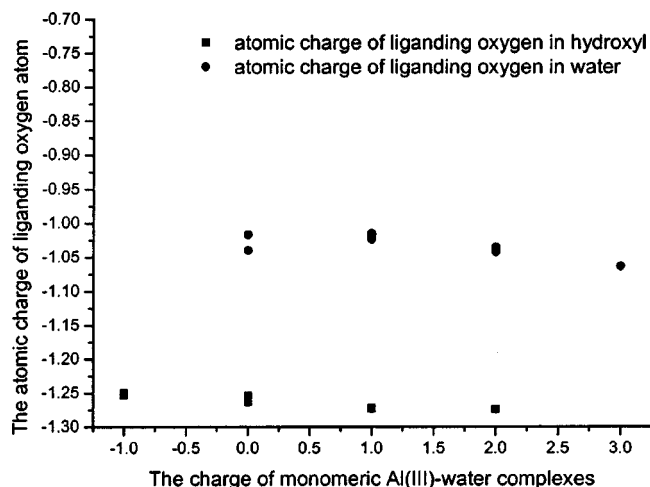


FIG. 2. The comparison between the atomic charge of liganding oxygen in hydroxyl and in water.

tions of their hydroxyl ligands. For the *cis/trans* isomers of $[\text{Al}(\text{H}_2\text{O})_4(\text{OH})_2]^+$ with respect to the relative position of hydroxyl ligands, differences in bond length for the Al—OH and Al—OH₂ bonds are much smaller than those among various monomeric Al(III) species with different charges (see Fig. 1). Their total energy difference is only 0.003 21 Hartree (8.44 kJ/mol), which indicates that they could easily convert to each other through protonation and deprotonation at room temperature. Figure 1 also shows that the bond lengths of Al—OH and Al—OH₂ are shortened almost linearly after an increase in the charge of complex, with the exception of the five-coordinate $[\text{Al}(\text{H}_2\text{O})_3(\text{OH})_3]^0$. The atomic charge of the ligating oxygen is larger in hydroxyl than it is in water (see Fig. 2), which may result in a stronger coordination interaction and affect their bridging properties during Al(III) polymerization. The optimized geometrical parameters and the total molecular energies for the selected model complex of the six monomeric Al(III) species are listed in Table I, and their optimized structures are shown in Fig. 3. The bond length of Al—OH in $[\text{Al}(\text{H}_2\text{O})_6]^{3+}$ is the same as Bock has reported at the same computational level.⁶ The results of Hessian calculations yielded all positive eigenvalues at the optimized geometry and confirmed that their structures are minima. The harmonic frequencies of *cis/trans* $[\text{Al}(\text{H}_2\text{O})_4(\text{OH})_2]^+$ are shown in Table II.

TABLE I. Optimized geometry parameters and the total energies of monomeric Al(III) complexes at the B3LYP/6-31G + (*d,p*) level.

Configuration	Geometrical parameters			NPA charges			Energy (hartree)
	$R(\text{Al-OH})/(\text{Å})$	$R(\text{Al-OH}_2)/(\text{Å})$	q_{Al}	q_{O}			
				OH	H ₂ O		
tet- $[\text{Al}(\text{OH})_4]^-$	1.792	N.A.	2.056	-1.253/-1.250	N.A.	-699.472 634 19	
$[\text{Al}(\text{H}_2\text{O})_3(\text{OH})_3]^0$	1.773	1.940	2.069	-1.254/-1.263	-1.017/-1.040	-699.472 634 19	
<i>cis</i> - $[\text{Al}(\text{H}_2\text{O})_4(\text{OH})_2]^+$	1.768	2.030	2.031	-1.273	-1.024/-1.017	-699.835 464 44	
<i>trans</i> - $[\text{Al}(\text{H}_2\text{O})_4(\text{OH})_2]^+$	1.765	2.020	2.038	-1.272	-1.015/-1.016	-699.838 671 92	
$[\text{Al}(\text{H}_2\text{O})_5\text{OH}]^{2+}$	1.719	1.975	2.049	-1.274	-1.035/-1.037/-1.043	-700.052 298 27	
$[\text{Al}(\text{H}_2\text{O})_6]^{3+}$	N.A.	1.942	2.076	N.A.	-1.064	-700.117 727 49	
$[\text{Al}(\text{H}_2\text{O})_6]^{3+a}$	N.A.	1.942	2.076	N.A.	-1.063	N.A.	

^aThe data obtained by Bock at the same computational level (Ref. 6).

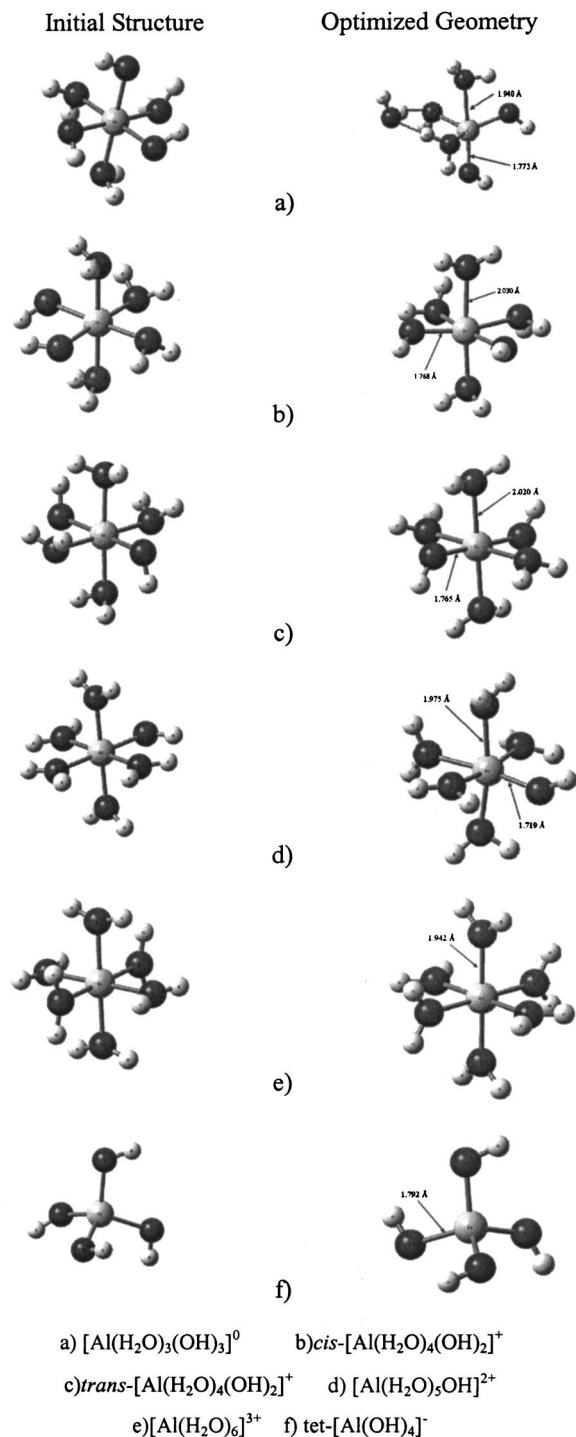


FIG. 3. Optimized structures of monomeric Al(III) water complexes at the B3LYP/6-31G + (d,p) level.

TABLE II. Calculated harmonic frequencies (in cm^{-1}) for the *cis/trans* $[\text{Al}(\text{H}_2\text{O})_4(\text{OH})_2]^+$ at the B3LYP/6-31G + (d,p) level of theory.

<i>cis</i> $[\text{Al}(\text{H}_2\text{O})_4(\text{OH})_2]^+$	<i>trans</i> $[\text{Al}(\text{H}_2\text{O})_4(\text{OH})_2]^+$
102, 141, 145, 179, 182, 213, 224, 248, 267, 277, 279, 287, 297, 314, 355, 363, 389, 397, 404, 517, 545, 597, 614, 626, 658, 666, 674, 687, 710, 795, 834, 1613, 1615, 1624, 1631, 3674, 3678, 3743, 3745, 3842, 3844, 3860, 3860, 3935, 3937	122, 134, 142, 187, 190, 208, 227, 268, 275, 286, 296, 308, 313, 318, 348, 350, 387, 401, 431, 480, 544, 576, 600, 603, 622, 652, 654, 684, 710, 896, 1600, 1601, 1612, 1617, 3719, 3719, 3765, 3767, 3866, 3866, 3883, 3884, 3955, 3955

The structure of monomeric hydroxyl Al(III) complexes is strongly related to the number of its hydroxyl ligands. The octahedral structure of monomeric Al(III) is stable with no more than two hydroxyl ligands. A large number of coordinating hydroxyls, such as in $[\text{Al}(\text{H}_2\text{O})_3(\text{OH})_3]^0$, distorts the geometry from its initial octahedron, with one water ligand leaving the first hydration sphere, followed by the monomer converting into a five-coordinate trigonal bipyramidal structure during the geometry optimization. This reduces the remarkable electrostatic repulsion between the hydroxyl ligands [see Fig. 3(a)]. This result is a little different from those obtained at the HF/3-21G level. However, if one takes into consideration the second hydration sphere, such as in the molecular cluster $[\text{Al}(\text{OH})_3] \cdot 9\text{H}_2\text{O}$, the trigonal bipyramidal structure is produced during the optimization process at the same theoretical level, with a very short bond length.²²

B. Dimeric aluminum complexes as a function of bridging ligand

1. The oxygen bridge

Oxygen bridged Al(III) dimers are proposed to exist in molten glass and in some extreme conditions such as in very basic solutions and at high temperatures.²³ To clarify the properties of the oxygen bridge group, both Al(III) atoms in each initial model dimer are octahedrally coordinated, and one of the two bridge ligands is simply an O^{2-} , while the other remains an OH^- ion. The calculated atomic charges of bridging oxygen ions in every cluster is listed in Table III and shown in Fig. 4. The initial and optimized geometries of the three complexes are shown in Fig. 5. Because the bridging oxygen has a high atomic charge of more than $1.4 e$, it is inclined to attract a proton through a hydrogen bond from one of the water molecules in the hydration sphere, while one of the water ligands is pushed out from the first hydration sphere of Al(III) during the structure optimization because of the strong electrostatic repulsion caused by the oxygen bridge group. Similar to the optimized monomeric Al(III) cluster $[\text{Al}(\text{H}_2\text{O})_3(\text{OH})_3]^0$, which has a high hydroxyl coordination number [see Fig. 3(a)], Al(III) clusters with an oxygen bridge ligand also appear to have trigonal bipyramidal geometry in all three dimeric complexes. This demonstrates that at a point when the electrostatic repulsive forces between its ligands become larger, the Al(III) water complex will prefer the trigonal bipyramidal geometry to an octahedral structure, to minimize this repulsive effect and stabilize itself.

TABLE III. Comparison of NPA charges for the oxygen atom at bridging position.

	$[\mu\text{-O}\cdot\mu\text{-OH}\cdot\text{Al}_2(\text{OH})_3(\text{H}_2\text{O})_5]^0$	$[\mu\text{-O}\cdot\mu\text{-OH}\cdot\text{Al}_2(\text{OH})_2(\text{H}_2\text{O})_6]^+$	$[\mu\text{-O}\cdot\mu\text{-OH}\cdot\text{Al}_2(\text{OH})_1(\text{H}_2\text{O})_7]^{2+}$
$q_{\mu\text{-O}}$	-1.447	-1.463	-1.449
$q_{\mu\text{-OH}}$	-1.243	-1.251	-1.261
	$[\mu\text{-H}_2\text{O}\cdot\mu\text{-OH}\cdot\text{Al}_2(\text{OH})_5(\text{H}_2\text{O})_3]^0$	$[\mu\text{-H}_2\text{O}\cdot\mu\text{-OH}\cdot\text{Al}_2(\text{OH})_2(\text{H}_2\text{O})_6]^{3+}$	$[\mu\text{-H}_2\text{O}\cdot\mu\text{-OH}\cdot\text{Al}_2(\text{OH})(\text{H}_2\text{O})_7]^{4+}$
$q_{\mu\text{-H}_2\text{O}}$	-1.053	-1.081	-1.102
$q_{\mu\text{-OH}}$	-1.249	-1.262	-1.245
	$[\mu\text{-H}_2\text{O}\cdot\mu\text{-OH}\cdot\text{Al}_2(\text{OH})_2(\text{H}_2\text{O})_6]^{3+}$	$[\mu\text{-H}_2\text{O}\cdot\mu\text{-OH}\cdot\text{Al}_2(\text{OH})_2(\text{H}_2\text{O})_6]^{3+}$	$[\mu\text{-H}_2\text{O}\cdot\mu\text{-OH}\cdot\text{Al}_2(\text{OH})(\text{H}_2\text{O})_7]^{4+}$
	$[\mu\text{-H}_2\text{O}\cdot\mu\text{-OH}\cdot\text{Al}_2(\text{OH})_2(\text{H}_2\text{O})_6]^{3+}$	$[\mu\text{-OH}\cdot\text{Al}_2(\text{OH})_2(\text{H}_2\text{O})_6]^{3+}$	$[\mu\text{-OH}\cdot\text{Al}_2(\text{OH})_2(\text{H}_2\text{O})_6]^{3+}$
	Al2-4w-0c-1 ^a	Al2-5w-1c-1 ^a	Al2-7w-3c-1 ^a
$q_{\mu\text{-OH}}$	-1.251/-1.239	-1.239/-1.240	-1.239/-1.251
	Al2-4w-0c-1 ^a	Al2-6w-2c-1 ^a	Al2-8w-4c-1 ^a
$q_{\mu\text{-OH}}$	-1.251/-1.239	-1.243/-1.246	-1.242/-1.254

^aThe double hydroxyl bridges complex (see Fig. 4).

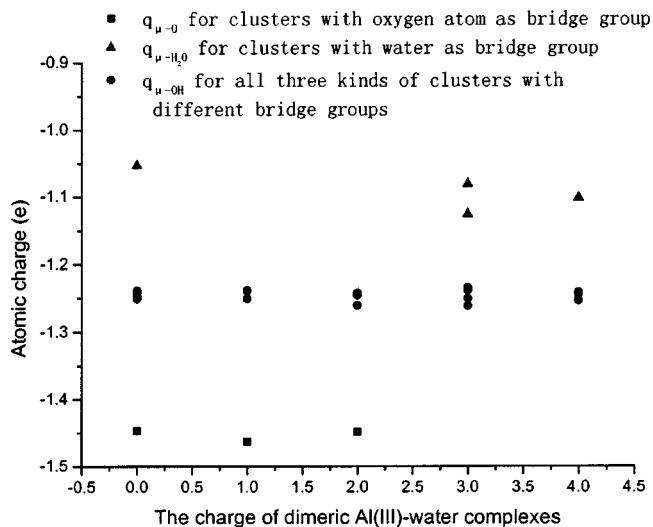


FIG. 4. Comparison of NPA charges for the oxygen atom at bridging position.

2. The water bridge

For comparison we have examined four dimeric model complexes that are bridged by water, a water and hydroxyl unit. These include $[\mu\text{-H}_2\text{O}\cdot\mu\text{-OH}\cdot\text{Al}_2(\text{OH})_5(\text{H}_2\text{O})_3]^0$, coplanar- $[\mu\text{-H}_2\text{O}\cdot\mu\text{-OH}\cdot\text{Al}_2(\text{OH})_2(\text{H}_2\text{O})_6]^{3+}$ (in the initial structure of this model complex, the three hydroxyl

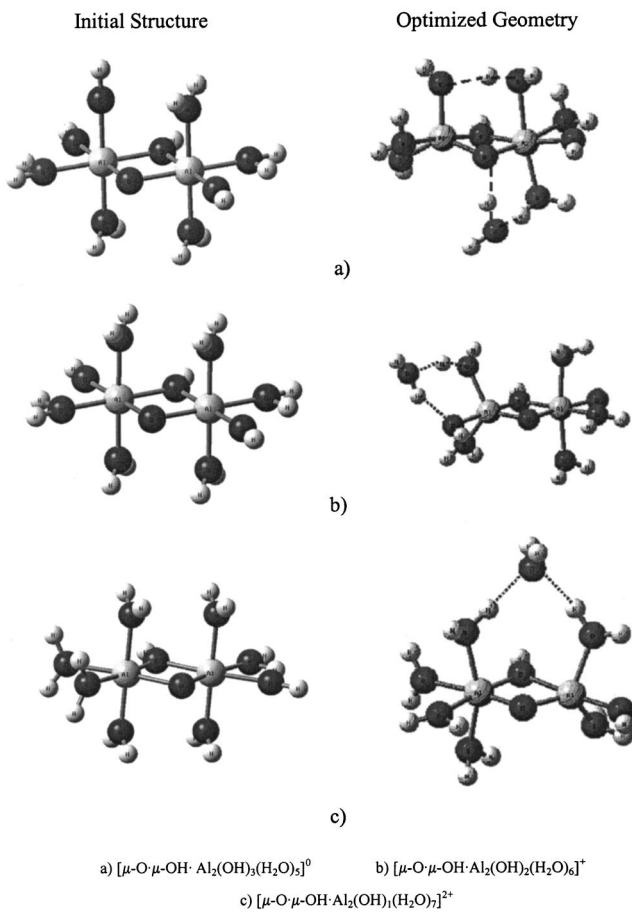


FIG. 5. Optimized structure of dimers with one oxygen ion bridge at the B3LYP/6-31G + (d,p) level.

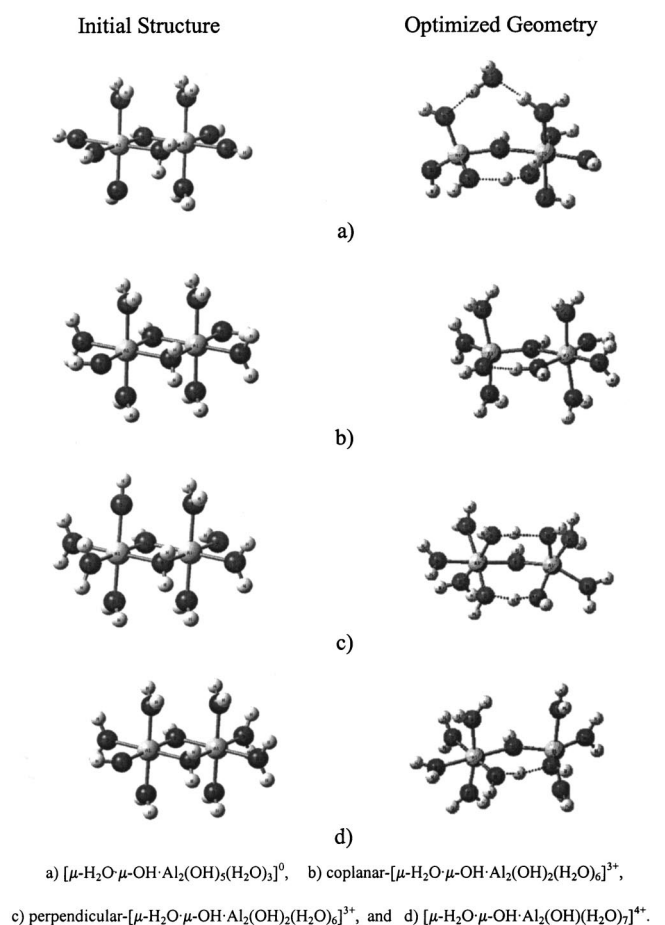


FIG. 6. Optimized dimeric Al(III) water complexes with one water bridge in the initial.

ligands are on the same plane), perpendicular- $[\mu\text{-H}_2\text{O}\cdot\mu\text{-OH}\cdot\text{Al}_2(\text{OH})_2(\text{H}_2\text{O})_6]^{3+}$ (in the initial structure of this model complex, the three hydroxyl ligands are perpendicular to each other), and $[\mu\text{-H}_2\text{O}\cdot\mu\text{-OH}\cdot\text{Al}_2(\text{OH})(\text{H}_2\text{O})_7]^{4+}$. In the dimers with a single bridging water, optimization revealed that they are not able to maintain their initial configuration and the broken water bridge becomes a ligand of the octahedral Al(III) ion. The low atomic charge of the oxygen in the bridging water indicates that it cannot provide enough negative charge to stabilize two Al(III). The optimized $[\text{Al}_2(\text{H}_2\text{O})(\text{OH})_6(\text{H}_2\text{O})_3]^0$ complex [see Fig. 6(a)] has a highly asymmetric configuration, with one Al tetrahedrally coordinated by four hydroxyls and the other remaining octahedrally coordinated. Meanwhile, we demonstrated again the formation of trigonal bipyramidal geometry for Al(III) with high hydroxyl coordination number in coplanar- $[\mu\text{-H}_2\text{O}\cdot\mu\text{-OH}\cdot\text{Al}_2(\text{OH})_2(\text{H}_2\text{O})_6]^{3+}$ [see Fig. 6(b)], perpendicular- $[\mu\text{-H}_2\text{O}\cdot\mu\text{-OH}\cdot\text{Al}_2(\text{OH})_2(\text{H}_2\text{O})_6]^{3+}$ [see Fig. 6(c)], and $[\mu\text{-H}_2\text{O}\cdot\mu\text{-OH}\cdot\text{Al}_2(\text{OH})(\text{H}_2\text{O})_7]^{4+}$ [see Fig. 6(d)].

3. Double hydroxyl bridges

Previous studies have shown that the hydroxyl is the most important bridging ligand for polyaluminum. The lowest energy dimeric Al(III) water complexes, with charges of 0, 1, 2, 3, and 4, are shown in Fig. 7. The hydroxyl ligand is

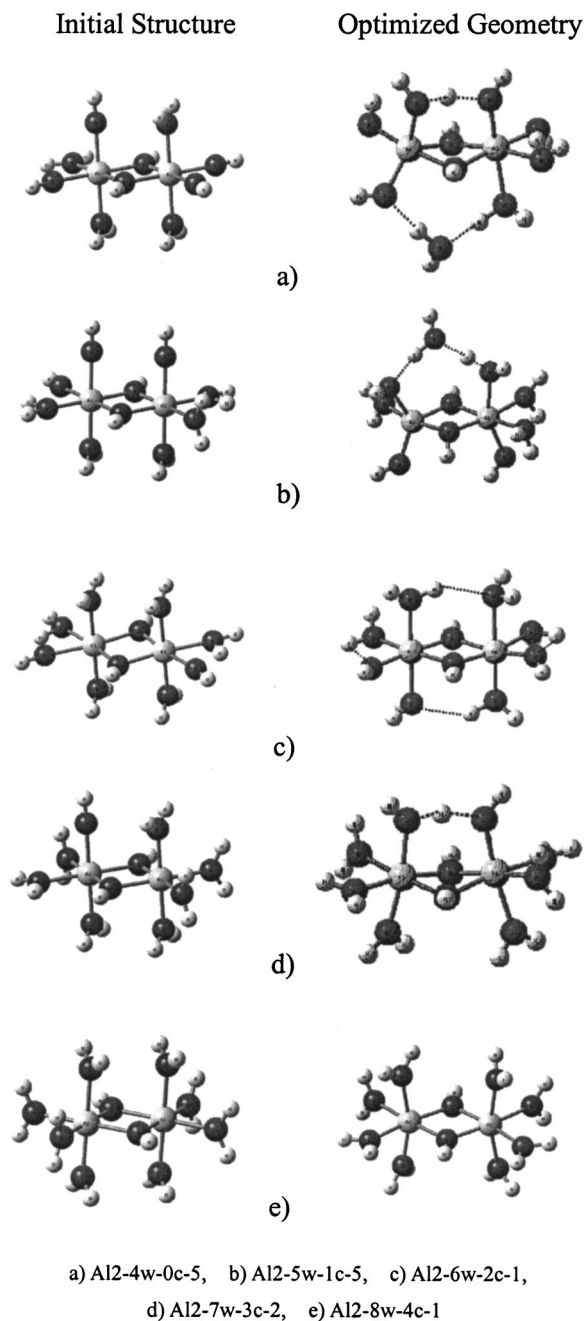


FIG. 7. Optimized structure of the minimum energy isomers with double hydroxyl bridging at the B3LYP/6-31G+(*d,p*) level.

shown to be a very stable bridging ligand, because of its low electron density compared with the oxygen ion and its suitable coordinate ability compared with the electronically neutral water (see Figs. 4 and 6). The trigonal bipyramidal geometry of five-coordinate Al(III) is again obtained in the optimized (Al2-4w-0c-5 and Al2-5w-1c-5) structures, which have high hydroxyl coordination numbers [see Figs. 7(a) and 7(b)].

To compare the stability of all possible isomers with two OH⁻ bridges, we considered the different arrangements of hydroxyl ligands with respect to the relative position of one another. The selected isomers were optimized at the B3LYP/6-31G+(*d,p*) level. Their calculated energies are listed in the Table IV. The results of Hessian calculations

TABLE IV. Optimized energy for double hydroxyl bridged dimeric Al(III) isomers using B3LYP method together with the 6-31G + (d,p).

Complex charge	Configuration	E (hartree)	ΔE^a (kJ mol ⁻¹)
0	Al2-4w-0c-1	-1 246.064 585 60	80.63
0	Al2-4w-0c-2	-1 246.088 833 19	16.97
0	Al2-4w-0c-3	-1 246.063 233 79	84.18
0	Al2-4w-0c-4	-1 246.087 676 62	20.00
0	Al2-4w-0c-5	-1 246.095 296 93	0
1	Al2-5w-1c-1	-1 246.479 935 81	7.828
1	Al2-5w-1c-2	-1 246.479 654 27	8.567
1	Al2-5w-1c-3	-1 246.478 950 70	10.41
1	Al2-5w-1c-4	-1 246.476 343 48	17.26
1	Al2-5w-1c-5	-1 246.482 917 17	0
1	Al2-5w-1c-6	-1 246.476 631 69	16.50
2	Al2-6w-2c-1	-1 246.739 771 62	0
2	Al2-6w-2c-2	-1 246.735 574 82	11.02
2	Al2-6w-2c-3	-1 246.738 560 94	3.179
2	Al2-6w-2c-4	-1 246.726 648 59	34.454
3	Al2-7w-3c-1	-1 246.851 109 86	53.87
3	Al2-7w-3c-2	-1 246.871 628 37	0
4	Al2-8w-4c-1	-1 246.853 479 68	0

^a ΔE is the energy difference between the isomer and the most stable complex with the same charge.

yielded all positive eigenvalues at the optimized geometry and confirmed that their structures are minima. The harmonic frequencies of all complexes shown in Fig. 7 are listed in Table V. From the optimized results shown in Table IV and Fig. 7, it is observed that those complexes with more hydrogen bonds are generally more stable (see Fig. 7). Moreover, those complexes whose negative hydroxyl ligands are in close proximity are generally more unstable from an energy perspective. This allows us to infer that the hydrogen bond is preferred in the stable isomers and that the electrostatic repulsive forces between hydroxyls are important in the formation of the polyaluminum structure. Our results also support

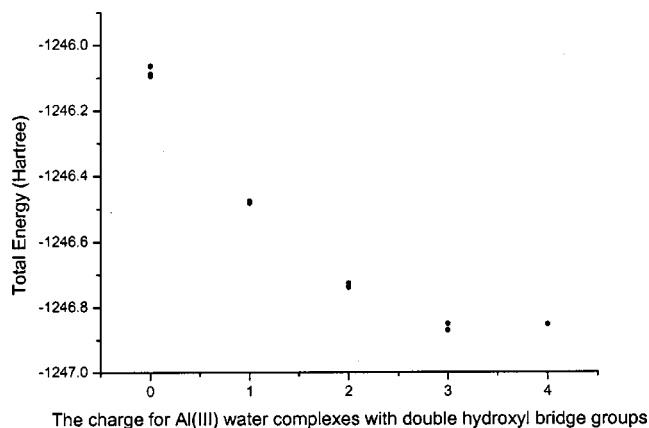


FIG. 8. The comparison of the total energy for all calculated Al(III) water complexes with double hydroxyl bridge groups.

Hem's experimental conclusion that polyaluminum shares only one doubly bridged OH group in a given plane.²⁴ Because the energy differences are less than 20 kJ mol⁻¹, these configurational isomers could coexist at room temperature (see Fig. 8).

We have also calculated the optimized geometries of OH-bridged polyaluminum isomers with negative charge. However, none of these maintained an octahedral structure. Some of them dissociated and divided into two separate Al anions during the geometry optimization.

C. Comparison of DFT and MP2

For the purpose of comparison, we performed several single-point MP2 calculations. To address this problem more clearly, only those structures with many hydrogen bonding were selected. In Table VI and Fig. 9, we show that the DFT

TABLE V. Calculated harmonic frequencies (in cm⁻¹) for all complexes shown in Fig. 7 at the B3LYP/6-31G + (d,p) level of theory.

Al2-4w-0c-5	Al2-5w-1c-5	Al2-6w-2c-1	Al2-7w-3c-2	Al2-8w-4c-1
60, 77, 83, 91, 119,	47, 62, 79, 99, 128,	76, 78, 107, 141,	76, 96, 100, 124,	36, 65, 66, 104,
143, 147, 170, 179,	136, 146, 162, 177,	167, 171, 174, 186,	134, 155, 157, 174,	106, 140, 149, 160,
195, 198, 213, 227,	185, 203, 221, 227,	215, 216, 221, 223,	191, 198, 201, 209,	168, 172, 178, 192,
253, 255, 261, 270,	240, 242, 254, 256,	242, 250, 257, 275,	212, 221, 251, 261,	204, 208, 212, 231,
296, 298, 322, 325,	267, 282, 289, 294,	287, 300, 311, 324,	272, 290, 303, 307,	241, 243, 254, 262,
340, 352, 364, 380,	310, 322, 327, 342,	325, 339, 346, 359,	318, 328, 336, 344,	268, 289, 305, 319,
395, 409, 432, 482,	354, 360, 383, 397,	366, 367, 397, 405,	355, 362, 381, 387,	325, 329, 352, 355,
490, 518, 523, 530,	414, 433, 472, 477,	406, 434, 451, 487,	392, 412, 435, 442,	364, 370, 410, 438,
540, 558, 569, 591,	491, 511, 534, 563,	512, 553, 565, 577,	448, 452, 465, 477,	444, 449, 452, 467,
608, 635, 650, 685,	583, 589, 597, 613,	579, 590, 598, 610,	481, 485, 492, 499,	493, 495, 518, 519,
708, 737, 738, 753,	643, 650, 663, 672,	633, 635, 659, 661,	531, 542, 562, 602,	531, 538, 545, 551,
762, 823, 852, 878,	699, 740, 769, 776,	675, 690, 697, 727,	613, 625, 649, 657,	561, 565, 579, 637,
882, 917, 942,	813, 847, 916, 947,	733, 805, 864, 946,	677, 694, 707, 721,	661, 666, 674, 699,
1152, 1184, 1657,	1018, 1231, 1572,	976, 1630, 1633,	858, 880, 987,	718, 728, 732, 758,
1667, 1671, 1720,	1608, 1616, 1634,	1633, 1634, 1657,	1005, 1302, 1460,	1029, 1069, 1671,
2206, 2925, 3145,	1717, 2517, 3149,	1660, 3674, 3675,	1642, 1645, 1648,	1672, 1679, 1681,
3557, 3801, 3852,	3603, 3738, 3759,	3688, 3690, 3697,	1651, 1670, 1671,	1685, 1685, 1689,
3856, 3869, 3873,	3839, 3855, 3859,	3698, 3802, 3802,	1870, 3719, 3722,	1694, 3672, 3686,
3881, 3908, 3929,	3880, 3880, 3882,	3823, 3824, 3831,	3723, 3726, 3740,	3687, 3698, 3699,
3942, 3947	3884, 3919, 3922,	3832, 3901, 3911,	3746, 3802, 3806,	3703, 3708, 3740,
	3955	3945, 3947	3810, 3815, 3818,	3741, 3755, 3755,
			3832, 3841, 3852,	3776, 3776, 3789,
			3854, 3856	3789, 3806, 3841

TABLE VI. The comparison of density functional theory and MP2.

	E(B3LYP) (hartree)	E(MP2) (hartree)
$[\text{Al}(\text{H}_2\text{O})_3(\text{OH})_3]^0$	-699.472 634 19	-696.579 586 05
$[\mu\text{-O}\cdot\mu\text{-OH}\cdot\text{Al}_2(\text{OH})_1(\text{H}_2\text{O})_7]^{2+}$	-1246.701 136 69	-1241.756 554 76
coplanar- $[\mu\text{-H}_2\text{O}\cdot\mu\text{-OH}\cdot\text{Al}_2(\text{OH})_2(\text{H}_2\text{O})_6]^{3+}$	-1246.842 376 12	-1241.912 075 30
Al2-8w-4c-1	-1246.853 479 68	-1241.939 334 98

and the MP2 methods produce quite similar results. Therefore, B3LYP should be a suitable method for this problem.

IV. CONCLUSION

Although it has been demonstrated that density Functional Theory can produce good results for the simulation of metal ions in water using cluster calculation,^{7,8} it is better to apply continuum models of solvation at MP2 level, which can calculate the proton transfer phenomena better, in order to simulate the behavior of polyaluminum. However, it is unrealistic to apply such a high theoretical level at present time. Within the limit of our computational level, we have achieved the following findings:

(1) Although the octahedral structures of hydroxyl aluminum predominate, the species with a smaller amount of charge or a large number of hydroxyl ligands has a tendency toward a five-coordinate trigonal bipyramid configuration.

(2) The electronically neutral water cannot provide enough negative charges to serve as a bridging ligand to stabilize two Al(III) ions.

(3) Even though so many configurational isomers of hydroxyl Al exist, their energy differences are limited, such that they may coexist and convert into each other easily at room temperature.

A figure for the optimized geometry of other dimeric aluminum water complexes can be found in EPAPS.²⁵

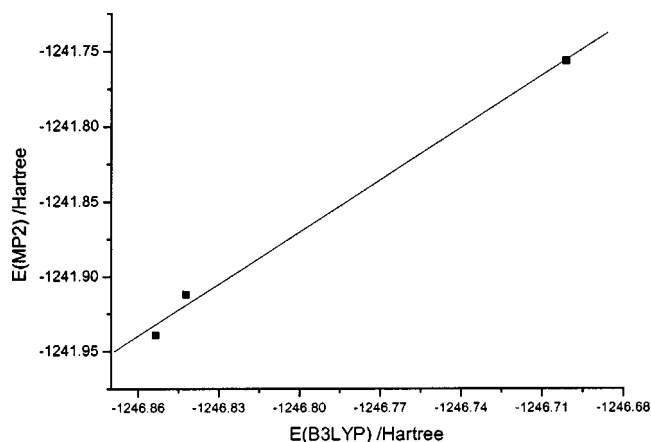


FIG. 9. The comparison of density functional theory and MP2.

ACKNOWLEDGMENTS

This project was supported by the National Science Foundation of China (Grant Nos. 20075011 and 49831005), Research Funding of National MOE of China for Young Teachers at Key University, Hwa-Ying Culture & Education Foundation of Nanjing University, and the Visiting Fellowship from the Berkeley Lawrence National Laboratory. We also thank the Computer Center of Nanjing University for computer time at the SGI 3800 and Dawning 3000 servers.

¹G. Sposito, *The Environmental Chemistry of Aluminum*, 2nd ed. (CRC, Boca Raton, Florida, 1995).

²D. Hunter and D. S. Ross, *Science* **251**, 1056 (1991).

³J. M. delaFuente, V. RamirezRodriguez, J. L. CabreraPonce, and L. HerreraEstrella, *Science* **276**, 1566 (1997).

⁴R. E. Connick and R. E. Poulson, *J. Am. Chem. Soc.* **79**, 5153 (1957).

⁵J. W. Akitt, N. N. Greenwood, B. L. Khandelwal, and G. D. J. Lester, *J. Chem. Soc. Dalton Trans.* **1972**, 604.

⁶C. W. Bock, G. D. Markham, A. K. Katz, and J. P. Glusker, *Inorg. Chem.* **42**, 1538 (2003).

⁷H. Erras-Hanauer, T. Clark, and R. van Eldik, *Coord. Chem. Rev.* **238–239**, 233 (2003).

⁸G. D. Markham, J. P. Glusker, and C. W. Bock, *J. Phys. Chem. B* **106**, 5118 (2002).

⁹M. I. Lubin, E. J. Bylaska, and J. H. Weare, *Chem. Phys. Lett.* **322**, 447 (2000).

¹⁰E. Wasserman, J. R. Rustad, and S. S. Xantheas, *J. Chem. Phys.* **106**, 9769 (1997).

¹¹J. M. Martinez, R. R. Pappalardo, and E. Sanchez Marcos, *J. Am. Chem. Soc.* **121**, 3175 (1999).

¹²T. Kowall, P. Caravan, H. Bourgeois, L. Helm, F. P. Rotzinger, and A. E. Merbach, *J. Am. Chem. Soc.* **120**, 6569 (1998).

¹³J. D. Kubicki, D. Sykes, and S. E. Apitz, *J. Phys. Chem. A* **103**, 903 (1999).

¹⁴A. E. Reed, R. B. Weinstock, and F. Weinhold, *J. Chem. Phys.* **83**, 735 (1985).

¹⁵M. J. Frisch, G. W. Trucks, H. B. Schlegel *et al.*, GAUSSIAN 98, Revision A.11, Gaussian, Inc., Pittsburgh, PA, 2001.

¹⁶P. C. Hariharan and J. A. Pople, *Theor. Chim. Acta* **28**, 213 (1973).

¹⁷A. D. Becke, *J. Chem. Phys.* **98**, 5648 (1993).

¹⁸C. Møller and M. A. Plesset, *Phys. Rev. A* **98**, 5612 (1993).

¹⁹C. Peng, P. Y. Ayala, H. B. Schlegel, and M. J. Frisch, *J. Comput. Chem.* **17**, 49 (1996).

²⁰A. E. Reed, L. A. Curtiss, and F. Weinhold, *Chem. Rev. (Washington, D.C.)* **88**, 899 (1988).

²¹A. E. Reed, R. B. Weinstock, and F. Weinhold, *J. Chem. Phys.* **83**, 735 (1985).

²²J. D. Kubicki, *J. Phys. Chem. A* **105**, 8756 (2001).

²³I. Farnan, *Nature (London)* **390(6655)**, 14 (1997).

²⁴J. D. Hem, *Am. Chem. Soc., Div. Water Waste Chem.* **7**, 54 (1967).

²⁵See EPAPS Document No. E-JCPSA6-121-303433 for optimized geometry of dimeric aluminum complexes. A direct link to this document may be found in the online article's HTML reference section. The document may also be reached via the EPAPS homepage (<http://www.aip.org/pubservs/epaps.html>) or from <ftp.aip.org> in the directory /epaps/. See the EPAPS homepage for more information.